Wang-Landau Monte Carlo formalism applied to ferroelectrics

S. Bin-Omran, Igor A. Kornev, and L. Bellaiche

Phys. Rev. B **93**, 014104 — Published 21 January 2016

DOI: 10.1103/PhysRevB.93.014104

Wang-Landau Monte-Carlo Formalism Applied to Ferroelectrics

S. Bin-Omran[1], Igor A. Kornev[2] and L. Bellaiche[3]

[1] *Department of Physics and Astronomy, King Saud University, Riyadh 11451, Saudi Arabia*

[2] *Laboratoire Structures, Propriétés et Modélisation des Solides, Université Paris-Saclay, CentraleSupélec, CNRS-UMR8580, Grande Voie des Vignes, 92295 Châtenay-Malabry Cedex, France*

[3] *Physics Department and Institute for Nanoscience and Engineering, University of Arkansas, Fayetteville, Arkansas 72701, USA*

Abstract

The Wang-Landau Monte Carlo algorithm is implemented within an effective Hamiltonian approach, and applied to $BaTiO_3$ bulk. The density of states obtained by this approach allows a highly-accurate and straightforward calculation of various thermodynamic properties, including phase transition temperatures, as well as polarization, dielectric susceptibility, specific heat and electrocaloric coefficient at any temperature. This approach yields rather smooth data even near phase transitions and provides a direct access to entropy and free energy, which allow to compute properties that are typically unaccessible by atomistic simulations. Examples of such latter properties are the nature (i.e., first-order *versus* second-order) of the phase transitions for different supercell sizes, and the thermodynamic limit of the Curie temperature and latent heat.

PACS numbers: 64.60.De,77.80.B-,77.70.+a,77.22.Ch,77.22.Ej

I. INTRODUCTION

Ferroelectric materials are of fundamental and technological interest. Over the past decades, numerical simulations based on the implementation of Metropolis Monte Carlo sampling or molecular dynamics methods[1,2] within atomistic approaches (e.g., effective Hamiltonians[3–6], bond valence and shell models[7,8]) have resulted in a better understanding of finite-temperature properties of ferroelectrics. Though they are widely used, standard Metropolis Monte Carlo and molecular dynamics methods encounter severe problems when applied to real ferroelectric systems. In particular, the critical slowing down near the phase transition temperature makes it very difficult to estimate the thermal average of some microscopic quantities with satisfactory accuracy in a reasonable computational time. For first-order transitions and for systems with rough energy landscapes, the Metropolis sampling and molecular dynamics methods may fail to sample configurations properly or even leave some configurations entirely unsampled. This kind of ergodicity breaking sometimes goes unnoticed, because it may show up clearly only in certain microscopic quantities. Moreover, Metropolis Monte Carlo methods and molecular dynamics methods do not typically give direct access to thermodynamic potentials. As a result, estimating the free energy or entropy from such methods is tricky [9,10], which makes the computation of some physical responses rather challenging.

Interestingly, a Monte Carlo method based on the density of states (or microcanonical ensemble partition function) proposed by Wang and Landau[11] has the potential to overcome these difficulties. As a matter of fact, the Wang-Landau (WL) algorithm has been successfully applied to numerous challenging problems in, e.g., magnetism[12,13], liquid crystals[14], biophysics[15], lattice gauge theories[16], etc. In particular, the WL method is useful for studying phase transition phenomena because it does not suffer from critical slowing. Surprisingly, it has been scarcely applied to the important class of materials formed by ferroelectrics, despite its potential (as evidenced by the the recent study of critical behavior in lead zirconate titanate materials using WL[17]). Three important issues therefore remain to be asserted, to the best of our knowledge, before definitely asserting the relevance of using WL to tackle complex phenomena in ferroelectrics: (1) is the WL algorithm able to reproduce with the same accuracy the finite-temperature properties that are already accessible by standard Monte-Carlo and Molecular Dynamics techniques in ferroelectrics (such

as temperature-driven transitions between the paraelectric and a ferroelectric state, or between ferroelectric states having different directions of the electrical polarization)? (2) Can the WL technique allows an easy access to an accurate computation of important physical responses that are directly linked to the free energy or entropy (such as electrocaloric coefficients) in ferroelectrics? (3) What type of insight (with respect to traditional Monte-Carlo or Molecular Dynamics) can the WL "bring to the table" in ferroelectrics?

The aim of this article is to address all these three general issues, by implementing the WL approach within a first-principles-derived effective Hamiltonian[3] to conduct a detailed study of physical properties of $BaTiO_3$. As we will see below, questions (1) and (2) can be positively answered. Moreover, the present study provides examples related to question (3), by, e.g., demonstrating that the character of ferroelectric phase transitions (i.e., second-order *versus* first-order) as well as several challenging quantities (such as the thermodynamic limit of the Curie point and latent heat) can be easily determined by using a WL algorithm within an atomistic approach.

The article is organized as follows. Section II provides details about the effective Hamiltonian and the Wang-Landau implementation. Results are given and discussed in Section III. Finally, Section IV summarizes the present work.

II. METHOD

A. Effective Hamiltonian

Here, we use the effective Hamiltonian (H_{eff}) of Ref.[3], that was developped to model $Ba_{1-x}Sr_xTiO_3$ (BST) systems. Its degrees of freedom are (1) the local soft mode $\mathbf{u}_i$[4], which is technically centered on the Ti-sites of the 5-atom unit cell i and which is directly proportional to the electric dipole moment of that cell; (2) inhomogeneous-strain-related dimensionless displacement variables $\{\mathbf{v}_i\}$[4]; and (3) the homogeneous strain tensor $\{\eta_H\}$[4]. Two additional physical quantities are defined in this effective Hamiltonian, but are kept frozen during the simulations – unlike $\{\mathbf{u}_i\}$, $\{\mathbf{v}_i\}$ and $\{\eta_H\}$. They are the set of variables $\{\sigma_j\}$ characterizing the atomic distribution of the mixed A-sublattice[6] – with σ_j=+1 or -1 corresponding to the presence of either Ba or Sr atom at the A-lattice site j – and the local strain $\{\eta_{\rm loc}\}$, which is related to the difference in ionic radius between Ba and Sr ions. The total internal energy

of this H_{eff} is given by:

$$E_{\rm tot} \;=\; E_{\rm ave}\left(\{\mathbf{u}_i\},\{\mathbf{v}_i\},\{\eta_H\}\right) + E_{\rm loc}\left(\{\mathbf{u_i}\},\{\mathbf{v}_i\},\{\sigma_j\},\{\eta_{\rm loc}\}\right). \qquad (1)$$

where $E_{\rm ave}$ represents the energy of a virtual $\langle A\rangle TiO_3$ simple system whose $\langle A\rangle$ atom involves the potential average of Ba and Sr atoms[18], and where $E_{\rm loc}$ represents a perturbation to this virtual crystal approximation to model real $(Ba_{1-x}Sr_x)TiO_3$ systems (including x=0, that is pure $BaTiO_3$). $E_{\rm ave}$ contains a local-mode self-energy, a long-range dipole-dipole interaction, a short-range interaction between soft modes, an elastic energy, and an interaction between the local modes and local strain[4]. Moreover, $E_{\rm loc}$ incorporates the effect of the real Ba and/or Sr ions on the local soft modes and the inhomogenous strain tensor[3]. All parameters of this effective Hamiltonian are fitted from first-principles calculations, except one of them (namely, the one related to the harmonic part of the local-mode self-energy) that is allowed to vary in order to reproduce the experimental value of the Curie temperature of disordered $(Ba_{0.5}Sr_{0.5})TiO_3$ solid solution. These parameters are provided in Ref.[3], and more details about effective Hamiltonians can be found in Ref.[4] (and references therein). When used in "traditional" Monte-Carlo (MC) and molecular dynamics techniques, this Hamiltonian has been shown to accurately predict several static and dynamical properties of BST systems[3,19,20,22]. In particular, it results in critical temperatures of 385, 280 and 230±5 K for the cubic-to-tetragonal, tetragonal-to-orthorhombic, and orthorhombic-to-rhombohedral transitions of pure $BaTiO_3$ (BTO) bulk, respectively, which are in good agreement with the corresponding measurements of 400K, 280K and 180K[23]. Other examples demonstrating the accuracy of this effective Hamiltonian is the subtle temperature-gradient-induced polarization[19], and the existence of two modes (rather than a single one, as previously believed for a long time) contributing to the GHz-THz dielectric response of $BaTiO_3$ and BST compounds[20,22].

B. Wang-Landau Method

Here, we implement the flat histogram sampling method of Wang and Landau[11] in Monte Carlo simulations using this effective Hamiltonian, and apply it to pure $BaTiO_3$ bulk, in order to illustrate how the resulting numerical tool can lead to a straightforward access of many properties that are usually rather challenging to compute or even model. This Wang-

Landau (WL) Monte Carlo simulation algorithm relies on the calculation of the density of states $\Omega(E)$, defined as the number of local dipole configurations for a given energy E. Unlike the conventional (Metropolis) Monte-Carlo method[1] that practically generates a canonical distribution $\Omega(E)\exp(-E/k_BT)$ at a given temperature, WL determines the density of states by conducting a non-markovian random walk in the configurational space. Specifically, in order to set up the energy histogram, one first obtains upper and lower bounds on E from estimating the energies relevant to a certain temperature interval. For cases (such as ferroelectrics) for which the energy can take continuous values, one needs to use a discretization scheme to divide the energy range of interest into a number of bins. Since $\Omega(E)$ is not known a priori, the histogram and $\Omega(E)$ are initialized with 0 and 1, respectively, for all energy bins between the upper and lower bounds. Then, the WL algorithm calculates $\Omega(E)$ in an iterative procedure by starting from a random local mode and strain configuration with energy in the range of interest. As the algorithm proceeds, the density of states is modified by a multiplicative factor and the energy histogram is simultaneously increased by 1 each time an energy bin is visited. The fact that the probability of the random walk is proportional to $1/\Omega(E)$ guarantees that the energy histogram becomes flat when all energy bins are about equally well sampled. In our simulations, the energy histograms are typically checked every 10^4 Monte-Carlo sweeps, and we impose the histogram of the lowest energy bin to be larger than 90% of the value of the energy histogram averaged over all energy bins as our criterion of flatness. The iteration is completed when flatness is achieved. Next, the modification factor is reduced following the strategy described in Ref.[21], the histogram is reset to zero for all bins, and the next step of iteration begins. Finally, the simulation ends after the modification factor has reached a sufficiently low value.

Once $\Omega(E)$ is determined, the partition function is naturally obtained for any temperature, T, as $Z = \Sigma_E \Omega(E) \exp(-\beta E)$ with $\beta = \frac{1}{k_B T}$. As a result and as we will now illustrate, many thermodynamic quantities can be easily calculated for *any* temperature, and in a single step, within WL.

III. RESULTS

For instance, the supercell average of any n power of the magnitude of the α-Cartesian component of the local modes can practically be determined by computing:

$$\langle |u_\alpha|^n \rangle = \frac{\Sigma_E |u_\alpha|^n \Omega(E) e^{-\beta E}}{\Sigma_E \Omega(E) e^{-\beta E}} \quad (2)$$

Note that such determination is similar in spirit with the computation of magnetic properties discussed in Refs.[12,13], since $|u_\alpha|^n$ is calculated here for each energy bin used for estimating $\Omega(E)$ rather than by considering the density of states as a function of both energy and polarization and then calculate this joint density of states (which is computationally demanding for ferroelectric systems).

A. Local modes and dielectric response

Figure 1a shows the temperature behavior of $\langle |u_\alpha| \rangle$, with α=x, y or z, as computed within WL using Eq.(2) with n=1, for a 16×16×16 $BaTiO_3$ supercell (note that the x, y and z axes are chosen along the pseudo-cubic [100], [010] and [001] directions, respectively). For comparison, Figure 1a also reports the computation of the supercell average of the local mode, $\langle \mathbf{u} \rangle$, for the same supercell, but using standard Metropolis Monte-Carlo simulations (using 20,000 MC sweeps for reaching thermal equilibrium and an additional 20,000 MC sweeps for computing statistical properties). It shows that the $\langle |u_x| \rangle, \langle |u_y| \rangle$ and $\langle |u_z| \rangle$ Cartesian components are all small at high temperature (note that they do not fully annihilate there because, unlike for the conventional MC simulations, Eq.(2), with n=1, corresponds to the computation of the supercell average of the *magnitude* of u_α rather than the supercell average of u_α – that can take positive *and* negative values. Such difference also explains why predicted critical transition temperatures can slightly vary between the WL and Metropolis algorithms). Figure 1a also shows that $\langle |u_z| \rangle$ suddenly increases, while $\langle |u_x| \rangle$ and $\langle |u_y| \rangle$ remain small, for temperatures below $\simeq$ 385K. This behavior is indicative that BTO bulk is predicted to undergo a phase transition from the paraelectric cubic phase to the ferroelectric tetragonal phase at the Curie temperature of $\simeq$ 385K, as similar to previous works using the same effective Hamiltonian but within Metropolis MC and molecular dynamics techniques[3,20,22]. Similarly, the sudden increase of $\langle |u_y| \rangle$ at around 280K and then of $\langle |u_x| \rangle$ close to 230K are characteristic of the well-known transitions towards (ferroelectric) orthorhombic and rhombohedral states, respectively. Figure 1a therefore attests that the implementation of the present H_{eff} within the WL algorithm is also capable of accurately predicting structural transitions in ferroelectric systems. Interestingly, the sharp increase of

the $\langle|u_\alpha|\rangle$'s seen in Fig. 1a at these three critical temperatures hint that the corresponding transitions are all first-order. We will come back to the nature of these transitions later on.

For now, let us concentrate on the diagonal elements of the dielectric response, $\chi_{\alpha\alpha}$, which can also be easily accessed from the Wang-Landau algorithm once $\Omega(E)$ is known, by computing[12,13]:

$$\chi_{\alpha\alpha} = \beta L^3(\langle|u_\alpha|^2\rangle - \langle|u_\alpha|\rangle^2) \tag{3}$$

for a L×L×L supercell, and where $\langle|u_\alpha|^2\rangle$ and $\langle|u_\alpha|\rangle$ are obtained via Eq.(2).

Figure 1b reports the average diagonal element of the dielectric tensor, i.e. $\chi_{diag} = \Sigma_\alpha\chi_{\alpha\alpha}/3$, as a function of temperature for the 16×16×16 supercell, and also compare it with the one obtained from the standard Metropolis Monte-Carlo simulations (this latter is computed from Eq. (3) too, but for which $\langle|u_\alpha|^2\rangle$ and $\langle|u_\alpha|\rangle$ are determined by averaging these quantities over the MC sweeps at every considered temperature). Figure 1(b) indicates that the WL algorithm correctly predicts peaks of χ_{diag} at the critical transition temperatures of 385, 280 and 230K, respectively. It is also important to realize that Fig. 1a and 1b demonstrate that one particular strength of the Wang-Landau algorithm is to provide physical quantity (such as polarization and dielectric response) that smoothly behave with temperature for any temperature window, which contrasts with the standard Metropolis Monte-Carlo simulations that typically yield large fluctuation near transition temperatures (see, e.g., the variation of u_x in Fig. 1a near 280K and χ_{diag} near 320K in Fig. 1b for the traditional MC computations). Such strength will be further demonstrated and taken advantage of below, and has been previously demonstrated to be crucial to study complex phenomena (such as the existence of critical behaviors in ferroelectric bulks or the diffuse character of phase transitions in ferroelectric ultrathin films[17,24]).

B. Specific heat

Note that other physical quantities can be naturally and smoothly obtained (for every temperature) by using the Wang-Landau algorithm. One example includes the specific heat, C, which is given within our WL implementation for a L×L×L supercell by [11–13]:

$$C = k_B\beta^2\frac{\langle E^2\rangle - \langle E\rangle^2}{L^3} \tag{4}$$

with

$$\langle E^n \rangle = \frac{\Sigma_E E^n \Omega(E) \exp(-\beta E)}{\Sigma_E \Omega(E) e^{-\beta E}} \tag{5}$$

for any n integer.

Figure 2a shows the resulting specific heat of $BaTiO_3$ as a function of temperature for a periodic supercell having lateral sizes of L=16. One can see sharp, large peaks at each transition temperature, which is consistent with the excess specific heat measured near the Curie temperature in Ref.[25] and with the fact that the three phase transitions of $BaTiO_3$ bulks are experimentally known to be of first order.

Let us know use one aforementioned strength of the WL method to further demonstrate that our effective Hamiltonian results for the specific heat are consistent with the known first-order nature of the paraelectric–to–ferroelectric transition in $BaTiO_3$ bulk. More precisely, we take advantage that WL provides very smooth data for the specific heat for any temperature and for any considered L×L×L supercell, as shown in Fig. 2b for temperatures close to the Curie point. Such smoothness allows to easily locate the Curie temperature (which is the position of the highest-temperature peak in the specific heat) and to extract the value of C at this Curie temperature for *any* studied L×L×L supercell. This latter value will be denoted here as C_L^{max}, and is shown in the inset of of Fig. 2b as a function of the L lateral size of the supercells (with L equal or larger than 12). This inset clearly reveals that C_L^{max} scales as L^3, which is fully consistent with finite-size scaling of a *first-order* transition[26].

Interestingly, the thermodynamic limit of the Curie temperature, $T_C(\infty)$, for the paraelectric-to-ferroelectric transition can also be easily determined within WL, by first identifying the transition temperature, $T_C(L)$, of the periodic L×L×L supercell as the maximum position of the specific heat and the minimum of the Binder parameter defined as $V(L) = 1 - \langle E^4 \rangle / 3(\langle E^2 \rangle)^2$ [26] (where $\langle E^4 \rangle$ and $\langle E^2 \rangle$ are given by Eq.(5) with n=4 and 2, respectively); and then using the finite-size scaling relation $T_C(\infty) - T_C(L) \sim L^{-3}$[26]. Doing so provides a $T_C(\infty)$ of 388.1 ± 0.1K for the presently used effective Hamiltonian.

C. Electrocaloric coefficient

Moreover, the electrocaloric coefficient, which is currently attracting a lot of attention[27–31] can also be "easily" extracted from the Wang-Landau algorithm at any temperature. For

that, one has to recall that the electrocaloric coefficient, γ, corresponds to a change of temperature under an applied electric field, $\mathcal{E}$, and is given by[30]:

$$\gamma = -\frac{T}{C}\left.\frac{\partial P}{\partial T}\right|_{\mathcal{E}} \tag{6}$$

where C is the specific heat and where P is the electrical polarization.

Taking C to be provided by Eq. (4) and $|P| = \frac{Z^*}{a_{lat}^2}\frac{\Sigma_E |\mathbf{u}|\Omega(E)e^{-\beta E}}{\Sigma_E \Omega(E)e^{-\beta E}}$, were Z^* and a_{lat} are the Born effective charge and the 5-atom lattice constant, respectively, gives in units of $\left[\frac{pK\cdot m}{V}\right]$:

$$\gamma = -1.945 Z^* a_{lat} L^3 T \left(\frac{\langle |\mathbf{u}|E\rangle - \langle |\mathbf{u}|\rangle\langle E\rangle}{\langle E^2\rangle - \langle E\rangle^2}\right) \tag{7}$$

where $\langle |\mathbf{u}|E\rangle = \frac{\sum_E |\mathbf{u}|E\Omega(E)\exp(-\beta E)}{\Sigma_E \Omega(E)e^{-\beta E}}$ and $\langle |\mathbf{u}|\rangle\langle E\rangle = \frac{\sum_E |\mathbf{u}|\Omega(E)\exp(-\beta E)}{\Sigma_E \Omega(E)e^{-\beta E}} \cdot \frac{\sum_E E\Omega(E)\exp(-\beta E)}{\Sigma_E \Omega(E)e^{-\beta E}}$, while $\langle E^2\rangle$ and $\langle E\rangle$ are given by Eq.(5).

Figure 2c shows the resulting electrocaloric coefficient for a 14×14×14 $BaTiO_3$ supercell, as computed from WL using Eq. (7). One can see that this coefficient peaks at the transition temperatures, as consistent with recent theoretical predications[28,29] and with measurements[32–34] in ferroelectric materials. In particular, γ is predicted to be larger than ∼50 mK.cm/kV in the vicinity of the Curie temperature, which is consistent with the experimental values of 53 mK.cm/kV obtained at a temperature of 391K in BTO polycrystal[32] and of 75 mK.cm/kV extracted at T=402 K in $BaTiO_3$ single crystal[33].

D. Example of insight provided by WL

Let us also now further demonstrate the type of physical insight that the WL method can provide in ferroelectrics, by, e.g, paying close attention to the paraelectric-to-ferroelectric transition in $BaTiO_3$ bulk. For that, we take advantage of the fact that the WL algorithm allows to compute the free-energy-like quantity defined as $A(E,\beta) = -\ln \mathcal{P}(E,\beta)$[35], where $\mathcal{P}(E,\beta) = \frac{\Omega(E)\exp(-\beta E)}{\Sigma_E \Omega(E)e^{-\beta E}}$ is the normalized canonical distribution (i.e., the canonical probability function). Figure 3a shows how A depends on the E internal energy for the 16×16×16 supercell and at three different temperatures that are all very close to the Curie temperature, namely 385.9, 385.0 and 384.0 K. A adopts two minima at energies to be denoted by E_f and E_p, respectively, for any of these three temperatures (with the value of E_f and E_p being slightly dependent on the temperature). Strikingly, the minimum of A at E_f is higher than the one at E_p for the temperature above 385K, while the opposite situation

holds below 385K and these two minima have equal depth at T=385K. Such features are representative of a first-order transition occurring at 385K (for L=16) with the minima at E_f and E_p corresponding to the equilibrium energy of the ferroelectric and paraelectric state, respectively. The first-order nature of the paraelectric-to-ferroelectic transition in $BaTiO_3$ is a known experimental feature, and is thus undoubtedly (and "easily") confirmed by the implementation of the Wang-Landau algorithm within our effective Hamiltonian. Interestingly, Figure 3b provides similar data at three temperatures close to T_C, but for the L×L×L supercell with $L = 10$ (note that the Curie temperature for such smaller supercell is numerically found to be 377.2K). In that case, the bimodality of the canonical probability distribution, and hence the double-well structure of A, is lost, i.e., there is only one minimum of A at any temperature (including the Curie temperature) – which is characteristic of *second-order* transitions. In other words, Figures 3a and 3b reveal that the (true) first-order nature of the paraelectric-to-ferroelectic transition in $BaTiO_3$ can only be resolved by simulations conducted on large-enough supercells (in our case, the L lateral size of this supercell has to be at least 12 unit cells).

Moreover, for any L×L×L supercell with L larger than 12, one can also extract the latent heat at the first-order paraelectric-to-ferroelectric transition as $\Delta e(L) = (E_f(L) - E_p(L))/L^3$, where the difference in energy between $E_f(L)$ and $E_p(L)$ is computed at the $T_C(\infty)$ critical temperature. The thermodynamic limit of this latent heat, $\Delta e(\infty)$, is then obtained by fitting the $\Delta e(L)$-*versus*-L curve as $\Delta e(L) = \Delta e(\infty) + a\exp(-bL)$, where a and b are parameters related to finite-size corrections (here, they are numerically found to be ≈ -1.2 J/g and ≈ 0.01 J/g, respectively). As shown in Fig. 3c, the resulting $\Delta e(\infty)$ is equal to 1.2 ± 0.05 J/g, which is in rather good agreement with the measurement of 1 J/g reported in Ref.[36]. The fact that $\Delta e(\infty)$ is finite is also fully consistent with the first-order character of the paraelectric–to-ferroelectric transition in $BaTiO_3$ bulk. Note that two previous methods also used effective Hamiltonian techniques within a special numerical procedure (namely, thermodynamic integration in Ref.[9] *versus* the application of auxiliary fields in Ref.[10]) to extract free-energy-like quantities close to the Curie temperature in $BaTiO_3$ bulk. However, these two methods did not report the behavior of free-energy-like quantity as a function of the internal energy, which therefore precluded the computation of the latent heat.

IV. SUMMARY

In summary, we have demonstrated the capabilities and advantages of combining the Wang-Landau Monte Carlo algorithm with an effective Hamiltonian approach for ferroelectric bulks. It is also important to realize that this WL scheme can be implemented within other atomistic approaches, such as the bond valence and shell models[7,8]. It can also be applied to *nanoscale* ferroelectrics, which are of high current interest – partly due to their potential applications in miniaturized devices[37–40]. In fact, it is timely and more appropriate to use the microcanonical ensemble (as automatically done within the WL algorithm) rather than the macrocanonical one (which is inherent to the Metropolis Monte-Carlo technique) when mimicking ferroelectric nanosystems[41,42]. We are therefore confident that our present work will motivate the use of the WL algorithm in ferroelectrics, both in their bulk and nanostructure forms, and can thus lead to a deeper understanding of this important class of materials as well as to the design of optimized or even novel properties.

This work is supported by the National Plan for Science, Technology and Innovation under the research project No. ADV-1498-02. L.B. thanks the financial support of DARPA grant HR0011-15-2-0038.

---

[1] N. Metropolis, A. W. Rosenbluth, M. N. Rosenbluth, A. H. Teller, and E. Teller, The Journal of Chemical Physics **21**, 1087 (1953).

[2] B. J. Alder and T. E. Wainwright, The Journal of Chemical Physics **27** (1957).

[3] L. Walizer, S. Lisenkov, and L. Bellaiche, Phys. Rev. B **73**, 144105 (2006).

[4] W. Zhong, D. Vanderbilt, and K. Rabe, Phys. Rev. Lett. **73**, 1861 (1994).

[5] U. V. Waghmare and K. M. Rabe, Phys. Rev. B **55**, 6161 (1997).

[6] L. Bellaiche, A. Garcia, and D. Vanderbilt, Phys. Rev. Lett. **84**, 5427 (2000).

[7] I. Grinberg, V.R. Cooper and A.M. Rappe, Nature (London) **419**, 144118 (2004).

[8] M. Sepliarsky, A. Asthagiri, S.R. Phillpot, M.G. Stachiotti and R.L. Migoni, Curr. Opin. Solid State Mater Sci. **9**, 107 (2005).

[9] G. Geneste, Phys. Rev. B **79**, 064101 (2009).

[10] J. Íñiguez, S. Ivantchev, J. M. Perez-Mato, and A. García, Phys. Rev. B **63**, 144103 (2001).

[11] F. Wang and D. P. Landau, Phys. Rev. Lett. **86**, 2050 (2001).

[12] B. J. Schulz, K. Binder, and M. Miller, International Journal of Modern Physics C **13**, 477 (2002).

[13] G. Brown and T. C. Schulthess, Journal of Applied Physics **97**, 10E303 (2005).

[14] D. Jayasri, V. S. S. Sastry, and K. P. N. Murthy, Phys. Rev. E **72**, 036702 (2005).

[15] N. Rathore and J. J. de Pablo, The Journal of Chemical Physics **116**, 7225 (2002).

[16] B. Bringoltz and S. R. Sharpe, Phys. Rev. D **78**, 074503 (2008).

[17] E. Almahmoud, I. Kornev, and L. Bellaiche, Phys. Rev. Lett. **102**, 105701 (2009).

[18] L. Bellaiche and D. Vanderbilt, Phys. Rev. B **61**, 7877 (2000).

[19] Q. Zhang and I. Ponomareva, Phys. Rev. Lett. **105**, 147602 (2010).

[20] I. Ponomareva, L. Bellaiche, T. Ostapchuk, J. Hlinka and J. Petzelt, Phys. Rev. B **77**, 012102 (2008).

[21] P. Poulain, F. Calvo, R. Antoine, M. Broyer, and Ph. Dugourd, Phys. Rev. E **73**, 056704 (2006).

[22] J. Hlinka, T. Ostapchuk, D. Nuzhnyy, J. Petzelt, P. Kuzel, C. Kadlec, P. Vanek, I. Ponomareva, and L. Bellaiche, Phys. Rev. Lett. **101**, 167402 (2008).

[23] C. Ménoret, J. M. Kiat, B. Dkhil, M. Dunlop, H. Dammak, and O. Hernandez, Phys. Rev. B **65**, 224104 (2002).

[24] S. Bin-Omran, I. Kornev, I. Ponomareva, and L. Bellaiche, Phys. Rev. B **81**, 094119 (2010).

[25] S. V. Grabovsky, I. V. Shnaidshtein, M. Takesada, A. Onodera, and B. A. Strukov, Journal of Advanced Dielectrics **03**, 1350032 (2013).

[26] K. Binder, ed., Monte Carlo Methods in Statistical Physics, Springer-Verlag (Springer, 1986).

[27] S. Prosandeev, I. Ponomareva and L. Bellaiche, Phys. Rev. B **78**, 052103 (2008).

[28] S. Lisenkov and I. Ponomareva, Phys. Rev. B **86**, 104103 (2012).

[29] M. C. Rose and R. E. Cohen, Phys. Rev. Lett. **109**, 187604 (2012).

[30] J. Scott, Annual Review of Materials Research **41**, 229 (2011).

[31] Y. Liu, I. C. Infante, X. Lou, L. Bellaiche, J. F. Scott, and B. Dkhil, Advanced Materials **26**, 6132 (2014).

[32] A. Karchevskii, Soviet Physics-Solid State **3**, 2249 (1962).

[33] X. Moya, E. Stern-Taulats, S. Crossley, D. Gonzlez-Alonso, S. Kar-Narayan, A. Planes, L. Maosa, and N. D. Mathur, Advanced Materials **25**, 1360 (2013).

[34] X. Moya, S. Kar-Narayan, and N. D. Mathur, Nature Materials **13**, 439 (2014).

[35] J. Lee and J. M. Kosterlitz, Phys. Rev. B **43**, 1268 (1991).

[36] Y. Bai, K. Ding, G.-P. Zheng, S.-Q. Shi, and L. Qiao, Physica Status Solidi (a) **209**, 941 (2012).

[37] J. F. Scott, F. D. Morrison, M. Miyake, and P. Zubko, Ferroelectrics **336**, 237 (2006).

[38] J. Varghese, R. W. Whatmore, and J. D. Holmes, J. Mater. Chem. C **1**, 2618 (2013).

[39] S. Prosandeev, I. Ponomareva, I. Naumov, I. Kornev, and L. Bellaiche, Journal of Physics: Condensed Matter **20**, 193201 (2008).

[40] S. Prosandeev, D. Wang, A. R. Akbarzadeh, and L. Bellaiche, Journal of Physics: Condensed Matter **27**, 223202 (2015).

[41] D. Gross, Microcanonical Thermodynamics: Phase Transitions in "small" Systems, World Scientific lecture notes in physics (World Scientific, 2001), ISBN 9789812798916.

[42] M. Pleimling and H. Behringer, Phase Transitions **78**, 787 (2005).

FIGURE CAPTIONS

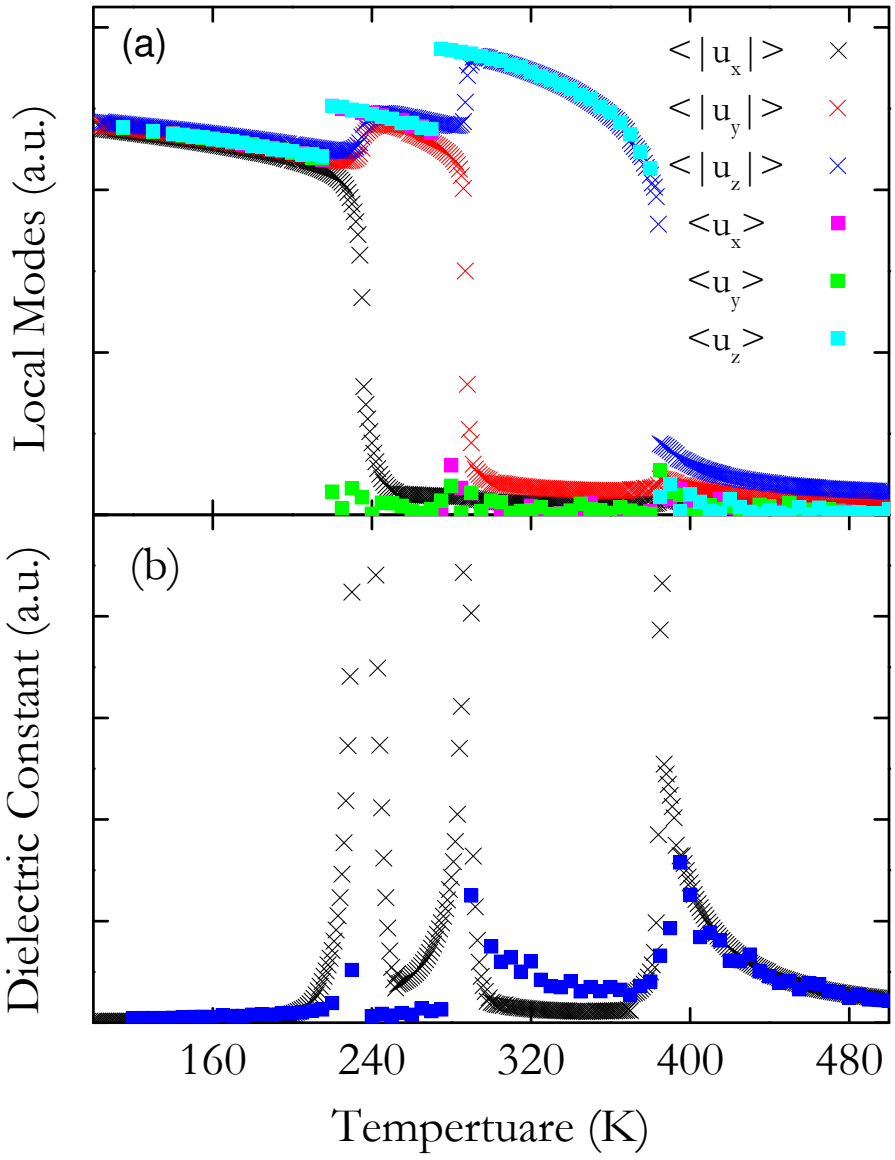

FIG. 1: Temperature behavior of the supercell average of the local mode (Panel a) and average dielectric susceptibility (Panel b) for a 16×16×16 periodic $BaTiO_3$ supercell, as predicted from the Wang-Landau method (crosses) and as computed using the Metropolis algorithm (squares).

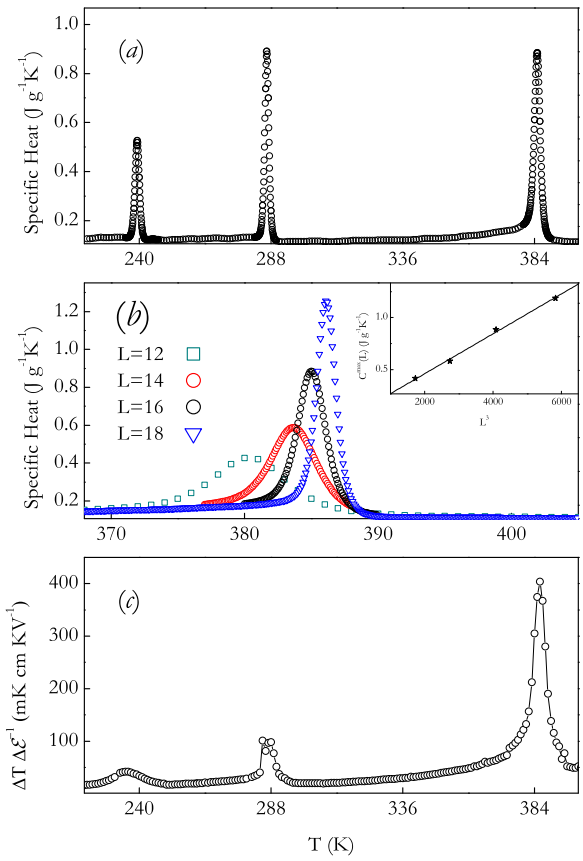

FIG. 2: Specific heat (Panels a and b) and electrocaloric coefficient (Panel c) *versus* temperature for periodic $BaTiO_3$ supercells, as computed within the Wang-Landau algorithm. Panel (a) shows the specific heat, C, of a $16\times16\times16$ periodic $BaTiO_3$ supercell for an interval of temperatures covering the three phase transitions while Panel (b) depicts C close to the paraelectric-to-ferroelectric transition for $L\times L\times L$ supercells having different L lateral sizes. The inset of Panel (b) shows C_L^{max} (see text) as a function of L^3, with the linear fit being represented by a straight line. A $14\times14\times14$ supercell is used for the results depicted in Panel (c). Error bars are smaller than the dimensions of the symbols.

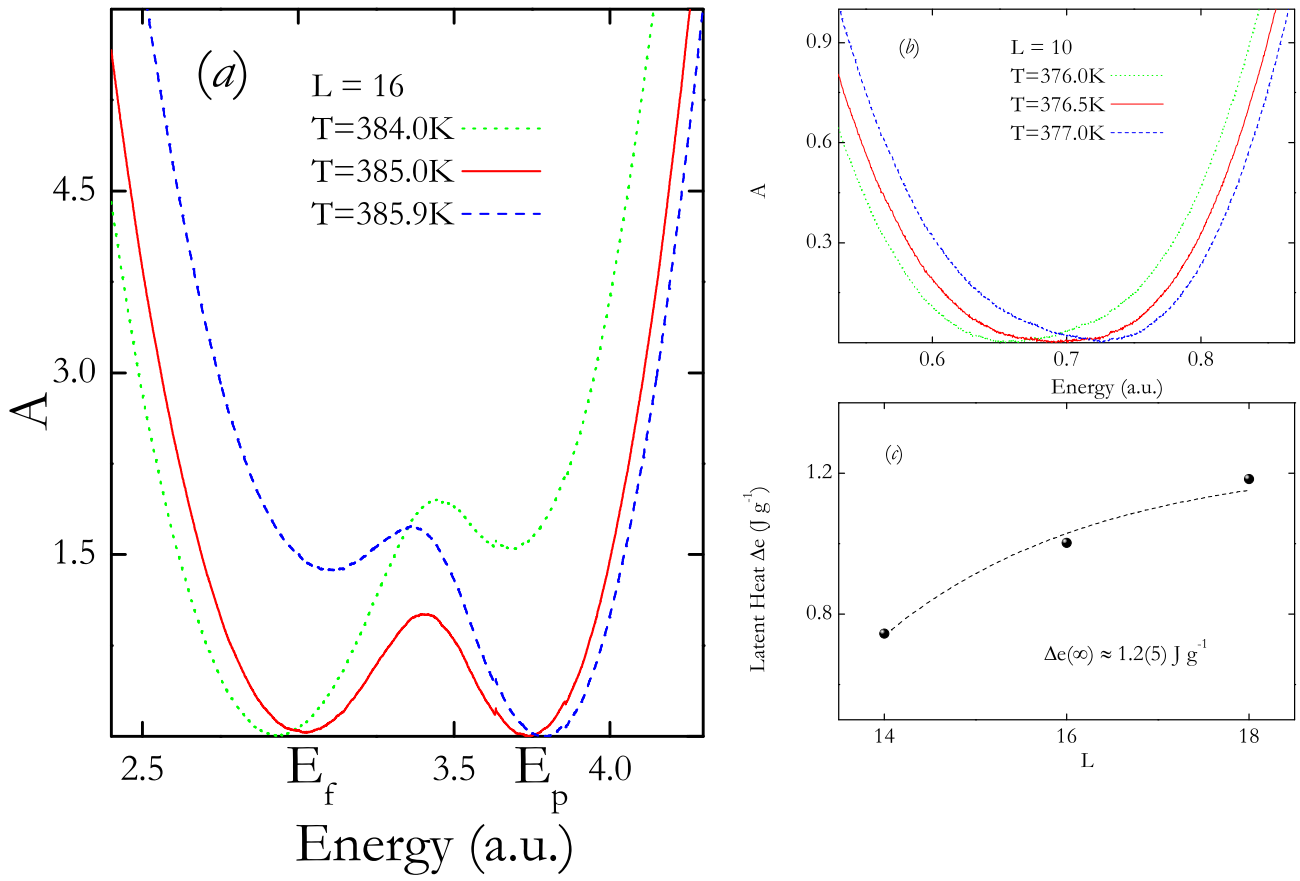

FIG. 3: Properties related to the nature of the paraelectric-to-ferroelectric transition of $BaTiO_3$ bulks, as obtained from the Wang-Landau algorithm. Panel (a) represents the free energy-like-quantity A *versus* the internal energy for temperatures above, below and at the transition point for a $16\times16\times16$ periodic $BaTiO_3$ supercell. Panel (b) provides similar data but for a $10\times10\times10$ supercell. Panel (c) displays the the finite-volume latent heat plotted against the lattice size L, with the fit to $\Delta e(L) = \Delta e(\infty) + a\exp(-bL)$ being shown via a dashed line.